

Zonally asymmetric ozone and the morphology of the planetary waveguide

John R. Albers¹, John P. McCormack², and Terrence R. Nathan¹

Abstract

Using a middle atmospheric general circulation model, we find that zonally asymmetric ozone (ZAO) profoundly changes the morphology of the Northern Hemisphere planetary waveguide (PWG). ZAO causes the PWG to contract meridionally and expand vertically, with a significant increase in wave propagation. Consequently, there is a significant increase in the upward flux of wave activity from the troposphere and lower stratosphere into the interior of the stratosphere and lower mesosphere. The ZAO-induced changes in the PWG increase the Eliassen-Palm flux divergence, causing a warmer and weaker stratospheric polar vortex. The ability of ZAO to alter the flux of planetary wave activity into the polar vortex has significant implications for accurately modeling wave-driven phenomena in the middle atmosphere, including sudden stratospheric warmings, 11-year solar cycle-modulated wave activity, and the Brewer-Dobson circulation.

1. Introduction

Understanding the physics that controls the planetary waveguide (PWG) is not fully understood; yet such understanding is vital to producing reliable assessments of human-caused impacts on key features of the climate system, including the upward flux of planetary wave activity, the frequency of stratospheric sudden warmings, and the Brewer-Dobson circulation. Here we demonstrate that the physics associated with zonally

¹ Department of Land, Air, and Water Resources: Atmospheric Science Program. University of California, Davis, CA, USA

² Space Science Division, Naval Research Laboratory, Washington D.C., USA

Report Documentation Page				Form Approved OMB No. 0704-0188	
Public reporting burden for the collection of information is estimated to average 1 hour per response, including the time for reviewing instructions, searching existing data sources, gathering and maintaining the data needed, and completing and reviewing the collection of information. Send comments regarding this burden estimate or any other aspect of this collection of information, including suggestions for reducing this burden, to Washington Headquarters Services, Directorate for Information Operations and Reports, 1215 Jefferson Davis Highway, Suite 1204, Arlington VA 22202-4302. Respondents should be aware that notwithstanding any other provision of law, no person shall be subject to a penalty for failing to comply with a collection of information if it does not display a currently valid OMB control number.					
1. REPORT DATE 15 JUL 2011		2. REPORT TYPE		3. DATES COVERED 00-00-2011 to 00-00-2011	
4. TITLE AND SUBTITLE Zonally asymmetric ozone and the morphology of the planetary waveguide				5a. CONTRACT NUMBER	
				5b. GRANT NUMBER	
				5c. PROGRAM ELEMENT NUMBER	
6. AUTHOR(S)				5d. PROJECT NUMBER	
				5e. TASK NUMBER	
				5f. WORK UNIT NUMBER	
7. PERFORMING ORGANIZATION NAME(S) AND ADDRESS(ES) Naval Research Laboratory, Space Science Division, 4555 Overlook Ave SW, Washington, DC, 20375				8. PERFORMING ORGANIZATION REPORT NUMBER	
9. SPONSORING/MONITORING AGENCY NAME(S) AND ADDRESS(ES)				10. SPONSOR/MONITOR'S ACRONYM(S)	
				11. SPONSOR/MONITOR'S REPORT NUMBER(S)	
12. DISTRIBUTION/AVAILABILITY STATEMENT Approved for public release; distribution unlimited					
13. SUPPLEMENTARY NOTES Geophysical Research Letters, submitted					
14. ABSTRACT Using a middle atmospheric general circulation model, we find that zonally asymmetric ozone (ZAO) profoundly changes the morphology of the Northern Hemisphere planetary waveguide (PWG). ZAO causes the PWG to contract meridionally and expand vertically, with a significant increase in wave propagation. Consequently, there is a significant increase in the upward flux of wave activity from the troposphere and lower stratosphere into the interior of the stratosphere and lower mesosphere. The ZAO-induced changes in the PWG increase the Eliassen-Palm flux divergence, causing a warmer and weaker stratospheric polar vortex. The ability of ZAO to alter the flux of planetary wave activity into the polar vortex has significant implications for accurately modeling wave-driven phenomena in the middle atmosphere, including sudden stratospheric warmings, 11-year solar cycle-modulated wave activity, and the Brewer-Dobson circulation.					
15. SUBJECT TERMS					
16. SECURITY CLASSIFICATION OF:			17. LIMITATION OF ABSTRACT Same as Report (SAR)	18. NUMBER OF PAGES 20	19a. NAME OF RESPONSIBLE PERSON
a. REPORT unclassified	b. ABSTRACT unclassified	c. THIS PAGE unclassified			

asymmetric ozone (ZAO) profoundly changes the morphology of the PWG, a result that underscores the importance of accurately accounting for ZAO in global climate models.

The concept of a PWG was first discussed by *Dickinson* [1968], who proposed that planetary waves would tend to propagate upward through the region of weak westerly winds bounded by the North Pole and the strong westerly winds of the stratospheric polar vortex. *Matsuno* [1970] derived a refractive index squared (RI) for planetary waves on a sphere and showed that while the large westerly wind speeds within the polar night jet may impede wave propagation, the vortex edge is characterized by strong meridional gradients in planetary vorticity that enhance wave propagation. Thus, rather than the polar vortex acting as the southern boundary of the waveguide, it is the tropical zero wind line that limits the equatorward propagation of planetary waves [*Tung*, 1979]. The PWG, therefore, is largely defined by the strength of wave propagation (measured by the RI) and its meridional width (measured by the location of the zero wind line). Mechanistic modeling studies have shown that diabatic effects due to ZAO modulate both of these and other wave-driven features in the tropics [*Echols and Nathan*, 1996; *Cordero and Nathan*, 1998, 2000] and extratropics [*Nathan and Li*, 1991; *Nathan et al.*, 1994; *Nathan and Cordero*, 2007].

For example, *Nathan and Cordero* [2007] derived an ozone-modified refractive index (OMRI) for vertically propagating planetary waves that describes how ZAO can produce changes in planetary wave propagation and wave attenuation (damping). Specifically, the OMRI makes clear how ZAO, which is a function of the vertical and horizontal gradients of background ozone, modulates planetary wave drag. Depending on

the background ozone gradients, planetary wave drag may either increase or decrease due to ZAO-induced changes in wave propagation and wave damping.

Evidence supporting the importance of ZAO in the stratosphere is not, however, limited to mechanistic studies. ZAO has also been shown to be important in altering the climate of general circulation models [e.g., *Sassi et al.*, 2005; *Gabriel et al.*, 2007; *Crook et al.*, 2008; *Waugh et al.*, 2009; *Gillett et al.*, 2009; *McCormack et al.*, 2011]. For example, *McCormack et al.* [2011] used a general circulation model with fully interactive ozone and dynamics to demonstrate that ZAO produces a warmer and weaker Northern Hemisphere stratospheric polar vortex, along with an increased incidence of SSWs.

Neither the mechanistic studies nor the general circulation model studies cited above have addressed the effects of ZAO on the PWG. Owing to the importance of accurately representing the PWG in global climate models, the goal of this paper is to examine how ZAO alters the morphology of the PWG of the Northern Hemisphere during winter. In the following section we introduce the model and diagnostics that we use to measure changes in the morphology of the PWG. We then present the results and follow with a discussion of the implications for global climate modeling.

2. Model Description and Diagnostics

We use the same model and experimental setup as in *McCormack et al.* [2011]. The effects of ZAO on planetary wave propagation during Northern Hemisphere winter are examined using the NOGAPS-ALPHA global spectral general circulation model [see, e.g., *Eckermann et al.*, 2009; *McCormack et al.*, 2009 and references therein], which extends from the surface to ~90 km in height and utilizes 68 hybrid (σ -p) vertical levels with triangular truncation at wavenumber 79. NOGAPS-ALPHA includes prognostic

equations for O_3 and H_2O calculated using the photochemical parameterizations of *McCormack et al.* [2006, 2008]. Shortwave heating and longwave cooling rates are computed using the predicted profiles of O_3 and H_2O , and a fixed profile of CO_2 . The lower boundary condition is computed from observed 12-hourly sea surface temperature and surface ice distributions.

In total, we ran fifteen pairs of simulations spanning early December to late March. Each pair of model simulations was initialized using identical profiles of wind, temperature, and chemical constituents acquired from the NOGAPS-ALPHA data assimilation system [*Eckermann et al.*, 2009]. The data we used for each pair of simulations was staggered in time in order to generate an ensemble of fifteen independent pairs of model simulations (for details see *McCormack et al.*, 2011). For each pair of simulations, one of the simulations utilized fully prognostic ozone in the radiative heating and cooling calculations (designated 3DO3), and the other simulation utilized zonal-mean ozone values to evaluate the radiative heating and cooling rates (designated ZMO3). Zonal-mean ozone values were calculated from the prognostic ozone field. We isolate the effect of ZAO on the circulation by taking the difference between 3DO3 and ZMO3 simulations for any given variable. Statistical significance between model variables was then assessed using a Student's T-test at the 95% confidence interval. As stated in *McCormack et al.* [2011], the 3DO3 model runs produced four SSWs, while the ZMO3 runs produced only one SSW. Statistical significance calculations were also carried out with all of the runs containing SSWs removed; however, doing so did not change the qualitative nature of our results.

The morphology of the PWG is evaluated in terms of two properties: i) its shape (meridional width and vertical extent); and ii) the strength of propagation within the guide itself. To diagnose the morphology of the PWG and to distinguish regions of wave propagation versus evanescence, we employ the spherical form of the quasigeostrophic refractive index squared (RI) [Andrews *et al.*, 1987]:

$$n_k^2(\phi, z) = \frac{\bar{q}_\phi}{\bar{u}} - \left(\frac{k}{a \cos \phi} \right)^2 - \left(\frac{f}{2NH} \right)^2, \quad (1)$$

where

$$\bar{q}_\phi = \frac{2\Omega \cos \phi}{a} - \frac{1}{a^2} \left(\frac{(\bar{u} \cos \phi)_\phi}{\cos \phi} \right) - \frac{f^2}{\rho_s} \left(\rho_s \frac{\bar{u}_z}{N^2} \right)_z \quad (2)$$

is the meridional potential vorticity gradient; ϕ is latitude, z is height, k is the zonal wavenumber, N is the buoyancy frequency, f is the Coriolis parameter, H is the mean scale height [=7 km], ρ_s is the sea-level reference density, a is the radius of the Earth, \bar{u} is the zonal mean zonal wind, Ω is the Earth's rotation frequency, and subscripts denote derivatives with respect to the given variable.

Planetary waves propagate within regions where $n_k^2 > 0$ and are evanescent in regions where $n_k^2 < 0$. Because $|n_k^2| \rightarrow \infty$ as $\bar{u} \rightarrow 0$, interpretation of the RI near the zero wind line becomes problematic. What is important here is that near the zero wind line the sign of \bar{u} largely controls the sign of n_k^2 . We therefore use the location of the zero wind line to approximate the southern boundary (and meridional width) of the PWG. Our use of the zero wind line as a measure of the southern boundary of the PWG is consistent with previous studies [e.g., Holton and Tan, 1982]. The vertical extent of the PWG and the strength of wave propagation within the waveguide are evaluated using the RI.

Moreover, if waves are assumed to be WKB in nature, then the local direction and magnitude of the vectors of the Eliassen-Palm flux (EP-flux) are also related to the RI (i.e., regions of larger RI are associated with larger EP-flux vectors) [Edmon *et al.*, 1980; Butchart *et al.*, 1982]. We plot EP-flux vectors at 100 hPa to assess how changes in wave propagation modulate the upward flux of wave activity into the middle and upper stratosphere. When plotting the EP-flux vectors, we adopt the scaling of Butchart *et al.* [1982] so that the EP-flux and its divergence are graphically consistent when plotted in Cartesian coordinates. We measure the net effect of changes in the zonal-mean circulation due to changes in the EP-flux divergence by the deceleration term defined in Palmer [1981] as

$$A_f = \frac{\exp(z/H)}{\rho_s a \cos \phi} \nabla \cdot \bar{\vec{F}}, \quad (3)$$

where $\nabla \cdot \bar{\vec{F}}$ is the EP-flux divergence and other variables are defined above.

3. Results

Figures 1a and 1b show the difference in the ensemble average zonal-mean zonal wind (3DO3 minus ZMO3) for January and February; wind differences that are statistically significant above the 95% confidence interval are shaded. Because the largest change in wind speed occurs in February in the Northern Hemisphere (NH), we focus our attention on this month and region for the remainder of the paper.

As Figure 1 shows, ZAO produces statistically significant decreases in the zonal mean westerly flow of 5-11 ms^{-1} in the equatorial upper stratosphere and middle mesosphere, as well as decreases of 3-18 ms^{-1} throughout the NH extratropical stratosphere and mesosphere. The difference in the NH zonal-mean wind produces two notable results. First, the decrease in the wind speed in the tropical upper stratosphere and

lower mesosphere causes a northward migration of the tropical easterlies and a northward shift of the zero wind line; the northward shift in the zero wind line varies from 1° to 8° latitude between 30 km and 65 km in height (Figure 2). Second, the decrease in wind speed within the extratropics and polar region represents a weaker polar vortex and a warmer stratosphere (see also *McCormack et al.* [2011], their Figure 2). These two changes in wind structure combine to modify the morphology of the PWG in distinct ways; the change in the location of the zero wind line narrows the width of the waveguide, while the change in the extratropical and polar winds expands the PWG in the vertical and strengthens wave propagation within the waveguide.

The meridional contraction of the PWG and the warmer, more disturbed polar vortex found in our results is in qualitative agreement with recent studies suggesting a connection between northward shifts in the upper stratospheric zero wind line and an increase in the frequency of SSWs. For example, *Gray* [2003] found that in a similar fashion to the so-called ‘Holton-Tan’ mechanism in the lower stratosphere [*Holton and Tan*, 1982], a northward shift in the upper stratospheric zero wind line produces a narrower waveguide that channels more wave activity poleward. The increase in wave activity induces more wave drag on the zonal-mean circulation and creates a warmer extratropical and polar stratosphere and an increased incidence of SSWs. Indeed, as our EP-flux diagnostics will show, the combination of a narrower PWG and an increase in wave propagation (discussed next) combine to produce an increase in wave activity and the weaker polar vortex shown in Figure 1b.

Figures 3a and 3b compare the contours of the February ensemble average RI (1) for ZMO3 and 3DO3 for stationary planetary wave ($s=1$); similar results were obtained

for planetary wave ($s=2$). The RI scale extends from red to blue, which corresponds with large to small RI values, respectively; regions where planetary waves are evanescent ($RI < 0$) are denoted by white space. Figure 3 shows that ZAO increases planetary wave propagation in two important ways. First, the vertical extent of the PWG increases, which allows the waves to propagate 10 to 15 km higher within the mesosphere between 50° - 70° . Second, ZAO causes a notable increase in the magnitude of the RI throughout the entire stratosphere. The latter point can be seen more easily by examining the difference in RI (3DO3 minus ZMO3) shown in Figure 3c. The change in the RI (Figure 3c) shows that ZAO produces a significant increase in wave propagation from ~ 15 km to 80 km in height between 30° - 70° north latitude. To better understand the implications of the expansion of the PWG in the vertical and the increase in wave propagation within the waveguide, we next consider the EP-flux and its divergence.

Figures 4a-c show contours of the EP-flux divergence in February for ZMO3, 3DO3, and the difference 3DO3 minus ZMO3. In addition, each of the EP-flux divergence contour plots is overlaid with the corresponding EP-flux vectors depicting the direction and relative magnitude of wave propagation at 100 hPa. The EP-flux vectors displayed in Figure 4 clearly show that ZAO causes an increase in the upward flux of wave activity between $\sim 30^\circ$ - 75° ; EP-flux vectors plotted at levels throughout the stratosphere show a similar increase due to ZAO. As expected, the increase in upward wave activity corresponds remarkably well with the increase in RI shown in Figure 3c. Moreover, the region of increased upward wave activity depicted by the EP-flux vectors is also associated with a larger and stronger region of EP-flux divergence below 30 km (Figure 4c). These results indicate that changes in wave propagation due to ZAO within

the lower stratosphere play an important role in modulating the amount of wave activity that is allowed to propagate from the troposphere into the interior of the stratosphere and lower mesosphere. The importance of the lower stratospheric changes in EP-flux and its divergence is further corroborated by considering the change in the zonal-mean deceleration (3). Figures 5a-c show the deceleration of the zonal-mean wind corresponding to the EP-flux divergence of Figure 4 for ZMO3, 3DO3, and the difference 3DO3 minus ZMO3. Indeed, Figure 5c shows a substantial net increase in the zonal-mean deceleration, A_f , due to ZAO. The increase in A_f correlates very well with both the expansion of the PWG in the vertical and the increase in wave propagation within the waveguide. The increase in A_f also corresponds very well with the decrease in the NH stratospheric and mesospheric zonal-mean wind profile shown in Figure 1b.

4. Conclusions and discussion

We investigated the effect of zonally asymmetric ozone (ZAO) on the zonal-mean circulation and planetary waveguide (PWG) of the Northern Hemisphere winter stratosphere and lower mesosphere using an ensemble of global circulation model (GCM) simulations. We demonstrated that ZAO profoundly alters the morphology of the PWG in two distinct ways. First, the PWG contracts meridionally and expands vertically within the upper stratosphere and lower mesosphere. Second, the magnitude of wave propagation increases throughout the interior of the stratospheric waveguide between $\sim 30^\circ$ - 75° . In combination, the changes in the shape and strength of the waveguide are associated with an increase in the deceleration of the zonal-mean circulation, a weaker and warmer stratospheric polar vortex, and an increased incidence of SSWs.

The modeled changes in the PWG have important implications for modeling SSWs, variations in stratospheric dynamics associated with the 11-year solar cycle, and the Brewer-Dobson circulation. For example, *Charlton et al.* [2007] investigated the ability of a series of GCMs – which did not consider the effects of ZAO on the PWG – to generate an accurate number of SSWs; the results showed that most GCMs failed to produce enough SSWs when compared to observations. In the current GCM study – where we explicitly consider the effects of ZAO on the PWG – the model runs with ZAO had a noticeably larger EP-flux at 100 hPa and produced a larger number of SSWs compared to similar runs without ZAO. This increase in the EP-flux correlates very well with the increase in the RI in the lower stratosphere, indicating that changes in the PWG associated with ZAO may play an important role in modulating the flux of wave activity entering the stratosphere from the troposphere, which is known to drive SSWs.

SSWs have also been correlated with northward shift of tropical easterlies and the zero wind line within the upper stratosphere and lower mesosphere [*Gray, 2003; Vineeth et al., 2010*]. *Gray et al.* [2003] suggested that because vertically propagating planetary waves have vertical wavelengths comparable to the distance between the tropopause and the upper stratosphere during mid- to late-winter, it is possible that shifts of the zero wind line in the upper stratosphere help to guide waves poleward in much the same manner as the traditional Holton-Tan mechanism in the lower stratosphere. Although our results have not tested the actual mechanics of this theory, it is nonetheless interesting to note the correlation between the northward shift in the zero wind line and the increase in frequency of SSWs in our model runs that include ZAO.

In addition to SSWs, two aspects of the PWG discussed in this study – the width and strength – may provide a means for ZAO to communicate and amplify the signal from the 11-year solar cycle. The relationship between the width of the PWG and solar-modulated ZAO has been shown by *Cordero and Nathan* [2005] to be an important pathway for communicating the solar signal to the QBO (see their Figure 1). Because our results show that ZAO plays a role in modulating the upper stratospheric tropical easterlies, it is therefore likely that in a similar manner to the *Cordero and Nathan* solar-QBO mechanism, ZAO may also play a role in modulating the semi-annual oscillation (SAO) in the tropical upper stratosphere. Because the SAO plays a dominant role in the location and timing of shifts in the upper stratospheric zero wind line, modulation of the SAO by ZAO may provide an important pathway for solar modulation of the width of the PWG. Indeed, this is a topic that deserves further attention given the parallel timing of the peak in wind modulation from ZAO in our results and the robust solar signal observed during mid- to late-winter in the tropical upper stratosphere [e.g., *Labitzke and van Loon*, 1988; *Naito and Hirota*, 1997]. In addition to solar modulation of the width of the waveguide, ZAO also provides a way to change the strength of wave propagation within the waveguide itself. This scenario is supported by recent work demonstrating the link between the 11-year solar cycle and changes in wave propagation and planetary wave drag in the extratropical stratosphere [*Nathan et al.*, 2011].

Finally, we note that recent modeling studies have projected that increasing greenhouse gas concentrations will affect stratospheric ozone abundance [*Eyring et al.*, 2007] and produce increases in wave activity that will accelerate the Brewer-Dobson circulation [*Garcia and Randel*, 2008]. Because ZAO is intimately connected to ozone

abundance and wave activity, ZAO may provide an important additional pathway for communicating greenhouse gas-induced changes in stratospheric ozone to the Brewer-Dobson circulation. We are currently investigating these possibilities.

Acknowledgments. JRA and TRN were supported in part by NSF grant ATM - 0733698 and by NASA/NRL grant NNH08AI67I. JPM was supported in part by the Office of Naval Research and in part by NASA Heliophysics Living with a Star TR&T Program award NNH08AI67I.

References

- Andrews, D. G., J. R. Holton, and C. B. Leovy (1987), *Middle Atmosphere Dynamics*, Elsevier, New York.
- Butchart, N., S. A. Clough, T. N. Palmer, P. J. Trevelyan (1982), Simulations of an observed stratospheric warming with quasigeostrophic refractive index as a model diagnostic, *Q. J. R. Meteorol. Soc.*, *108*, 475-502.
- Charlton, A. J., et al. (2007), A new look at stratospheric sudden warmings. Part II: Evaluation of numerical model simulations, *J. Clim.*, *20*, 470-488.
- Cordero, E. C., and T. R. Nathan (1998), An analytical study of ozone feedbacks on Kelvin and Rossby-Gravity waves: Effects on the QBO, *J. Atmos. Sci.*, *55*, 1051-1062.
- Cordero, E. C., and T. R. Nathan (2000), The influence of wave- and zonal mean-ozone feedbacks on the quasi-biennial oscillation, *J. Atmos. Sci.*, *57*, 3426-3442.
- Cordero, E. C., and T. R. Nathan (2005), A new pathway for communicating the 11-year solar cycle signal to the QBO, *Geophys. Res. Lett.*, *32*, L18805.
- Crook, J. A., N. P. Gillett, and S. P. Keeley (2008), Sensitivity of Southern Hemisphere climate to zonal asymmetry in ozone, *Geophys. Res. Lett.*, *35*, L07806.

- Dickinson, R. E. (1968), Planetary Rossby waves propagating vertically through weak westerly wave guides, *J. Atmos. Sci.* 25, 984-1002.
- Echols, R. S., and T. R. Nathan (1996), Effects of ozone heating on forced equatorial Kelvin waves, *J. Atmos. Sci.* 53, 263-275.
- Eckermann, S. D., et al. (2009). High-altitude data assimilation system experiments for the Northern Hemisphere summer mesosphere season of 2007, *J. Atmos. Sol. Terr. Phys.*, 71, 531-551.
- Edmon, H. J., B. J. Hoskins, M. E. McIntyre (1980), Eliassen-Palm cross sections for the troposphere, *J. Atmos. Sci.*, 37, 2600-2616.
- Eyring, V., et al. (2007), Multimodel projections of stratospheric ozone abundance in the 21st century, *J. Geophys. Res.*, 112, D16303.
- Gabriel, A., D. Peters, I. Kirchner, and H. F. Graf. (2007), Effect of zonally asymmetric ozone on stratospheric temperature and planetary wave propagation, *Geophys. Res. Lett.*, 34, L06807.
- Garcia, R. R. and W. J. Randel (2008), Acceleration of the Brewer-Dobson circulation due to increases in greenhouse gases, *J. Atmos. Sci.*, 65, 2731-2739.
- Gillett, N. P., J. F. Scinocca, D. A. Plummer, M. C. Reader (2009), Sensitivity of climate to dynamically-consistent zonal asymmetries in ozone, *Geophys. Res. Lett.*, 36, L10809.
- Gray, L. J. (2003), The influence of the equatorial upper stratosphere on stratospheric sudden warmings, *Geophys. Res. Lett.*, 30, L041166.
- Holton, J. R. and H.C. Tan (1982), The quasi-biennial oscillation in the Northern Hemisphere lower stratosphere, *J. Meteor. Soc. Japan*, 60, 140-148.

- Labitzke, K., and H. van Loon (1988), Association between the 11-year solar cycle, the QBO, and the atmosphere. Part I: The troposphere and stratosphere on the Northern Hemisphere winter, *J. Atmos. Terr. Phys.*, *50*, 197-206.
- Matsuno, T. (1970), Vertical propagation of stationary planetary waves in the winter Northern Hemisphere, *J. Atmos. Sci.* *27*, 871-883.
- McCormack, J. P., S. D. Eckermann, D. E. Siskind, and T. J. McGee (2006), CHEM2D-OPP: A new linearized gas-phase ozone photochemistry parameterization for high-altitude NWP and climate models, *Atmos. Chem. Phys.*, *6*, 4943-4972.
- McCormack, J. P., K. H. Hoppel, and D. S. Siskind (2008), Parameterization of middle atmospheric water vapor photochemistry for high-altitude NWP and data assimilation, *Atmos. Chem. Phys. Discuss.*, *8*, 13999-14032.
- McCormack, J. P., L. Coy, and K. W. Hoppel (2009), Evolution of the quasi 2day wave during January 2006, *J. Geophys. Res.*, *114*, D20115.
- McCormack, J. P., T. R. Nathan, and E. C. Cordero (2011), The effect of zonally asymmetric ozone heating on the Northern Hemisphere winter polar stratosphere, *Geophys. Res. Lett.*, *38*, L03802.
- Naito, Y., and I. Hirota (1997), Interannual variability of the northern winter stratospheric circulation related to the QBO and the solar cycle, *J. Meteorol. Soc. Japan*, *75*, 925-937.
- Nathan, T. R., and L. Li (1991), Linear stability of free planetary waves in the presence of radiative-photochemical feedbacks, *J. Atmos. Sci.* *48*, 1837-1855.
- Nathan, T. R., E. C. Cordero, and L. Li (1994), Ozone heating and the destabilization of traveling waves during summer, *Geophys. Res. Lett.* *21*, 1531-1534.

- Nathan, T. R., and E. C. Cordero (2007), An ozone modified refractive index for vertically propagating planetary waves, *J. Geophys. Res.*, *112*, D02105.
- Nathan, T. R., J. R. Albers, and E. C. Cordero (2011), Role of wave-mean flow interaction in sun-climate connections: Historical overview and some new interpretations and results, *J. Atmos. Sol. Terr. Phys.*, in press.
- Palmer, T. N. (1981), Diagnostic study of a wavenumber-2 stratospheric sudden warming in a transformed Eulerian-mean formalism, *J. Atmos. Sci.*, *38*, 844-855.
- Sassi, F., B. A. Boville, D. Kinnison, R. R. Garcia (2005), The effects of interactive ozone chemistry on simulations of the middle atmosphere, *Geophys. Res. Lett.*, *32*, L07811.
- Tung, K. K. (1979), A Theory of stationary long waves. Part III: Quasi-normal modes in a singular waveguide, *J. Atmos. Sci.* *107*, 751-774.
- Vineeth, C., T. K. Pant, K. K. Kumar, S. G. Sumod (2010), Tropical connection to the polar stratospheric sudden warming through quasi 16-day planetary wave, *Ann. Geophys.* *28*, 2007-2013.
- Waugh, D. W., L. Oman, P. A. Newman, R. S. Stolarski, S. Pawson, J. E. Nielsen, and J. Perlwitz (2009), Effects of zonal asymmetries in stratospheric ozone on simulated Southern Hemisphere climate trends, *Geophys. Res. Lett.*, *36*, L1870.

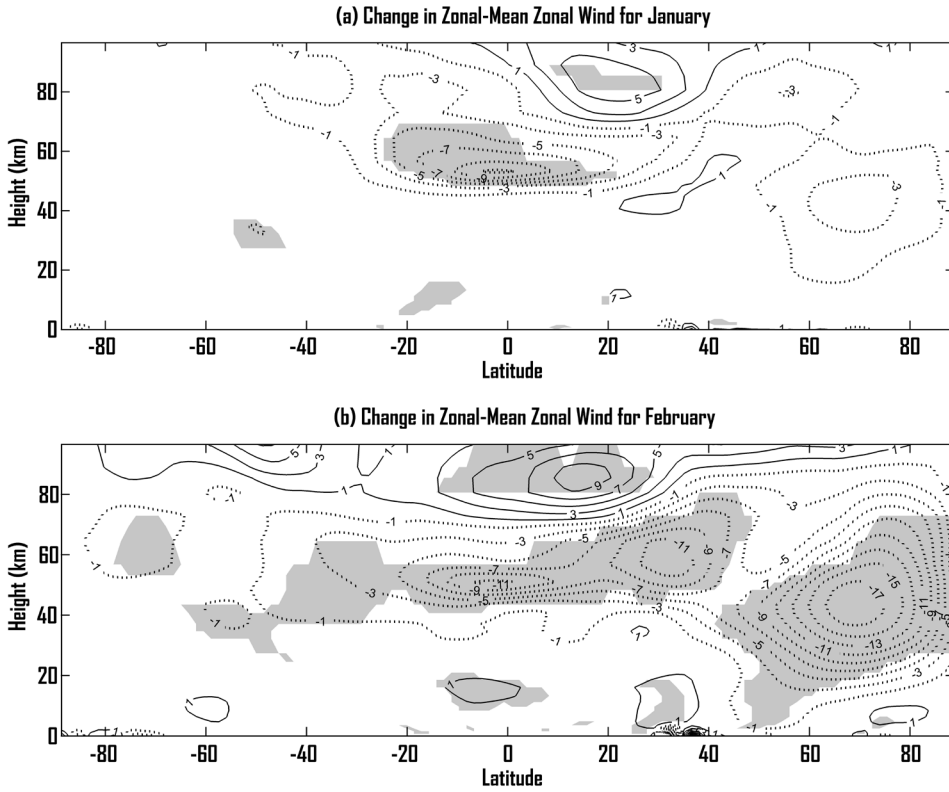


Figure 1. Monthly average zonal-mean zonal wind difference ($\Delta U = 3DO3$ minus $ZMO3$) for: (a) January and (b) February. Contours intervals noted in the Figure are in units of ms^{-1} . Statistically significant wind changes at the 95% confidence interval are shaded in gray.

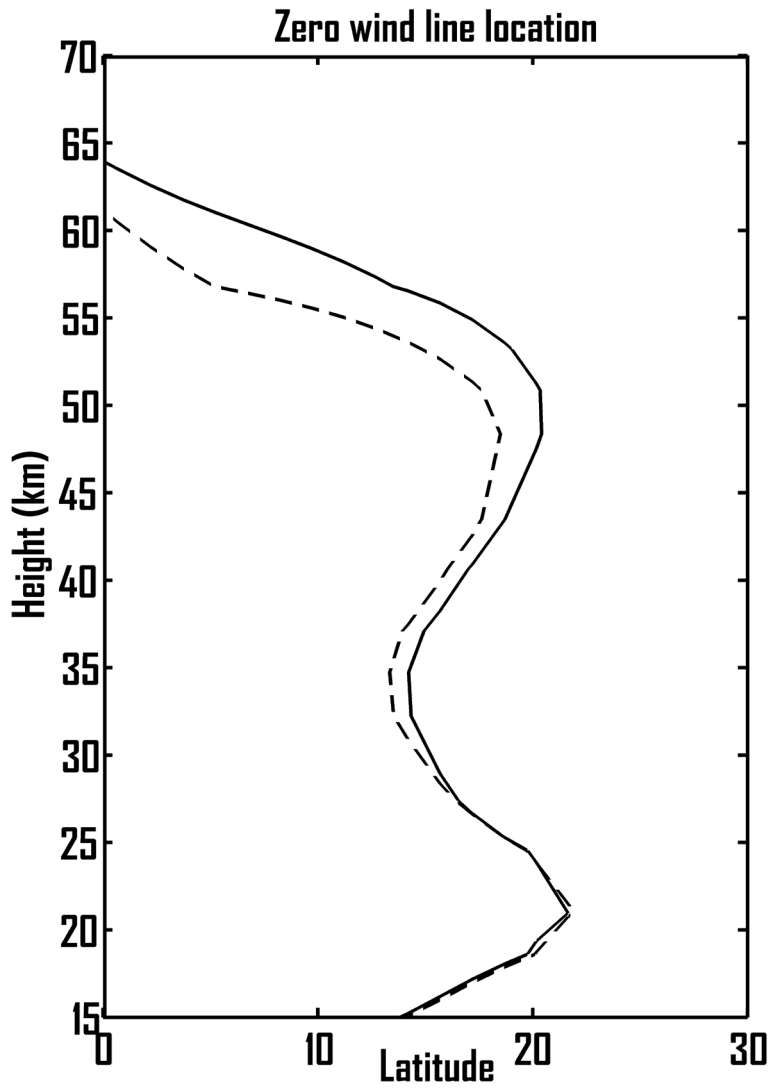


Figure 2. Location of Northern Hemisphere zero wind line for 3DO3 (solid line) and ZMO3 (dashed line).

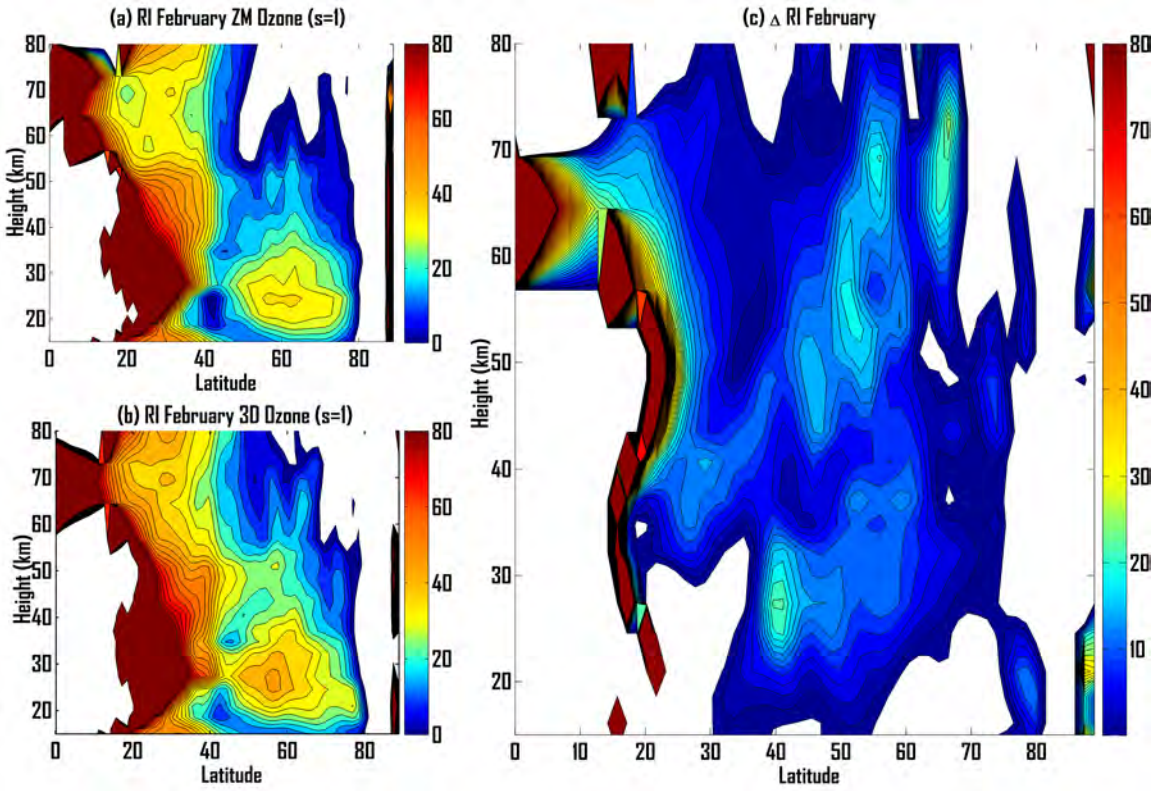


Figure 3. Monthly averaged refractive index squared (RI) in February for: (a) ZMO3 for planetary wave $s=1$; (b) 3DO3 for planetary wave $s=1$; and (c) difference in RI ($\Delta RI = 3DO3$ minus $ZMO3$). Regions of wave evanescence ($RI < 0$) are depicted by regions without shading (white). In all plots, the RI has been multiplied by α^2 ; the contour interval is 4.

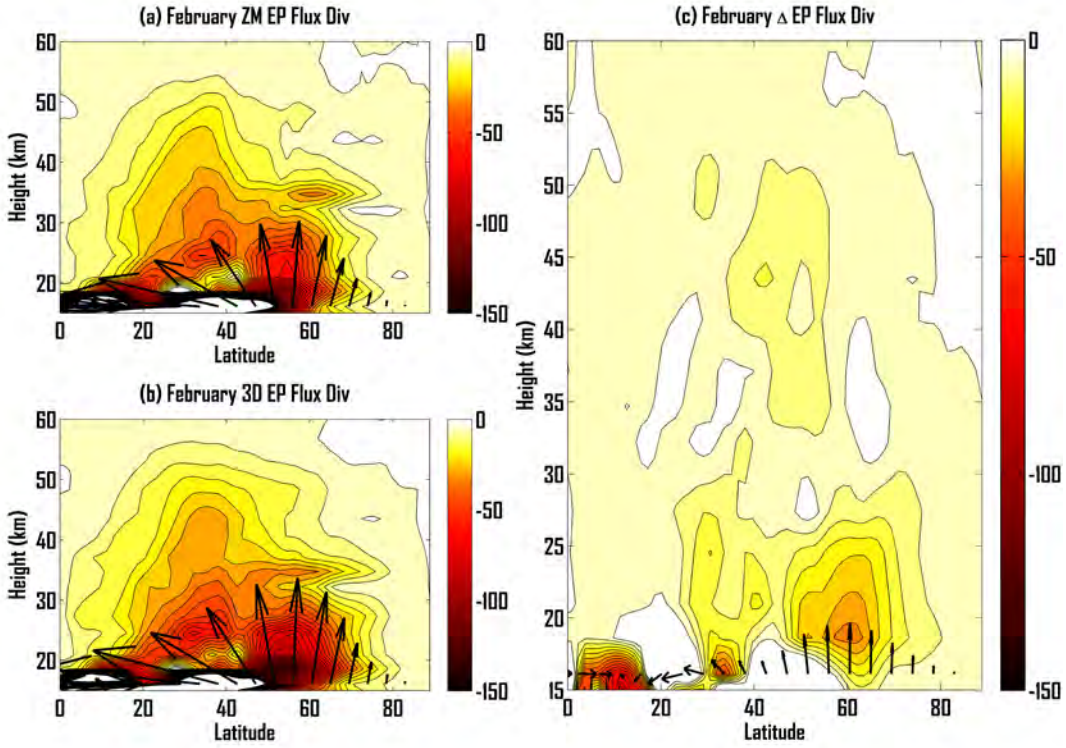


Figure 4. Monthly averaged EP-flux divergence in February for: (a) ZMO3; (b) 3DO3; and (c) difference in EP-flux divergence (3DO3 minus ZMO3). Arrows represent EP-vectors plotted at the 100 hPa height level (~16 km). The contour interval is $5 \times 10^{-6} \text{ kg s}^{-2}$.

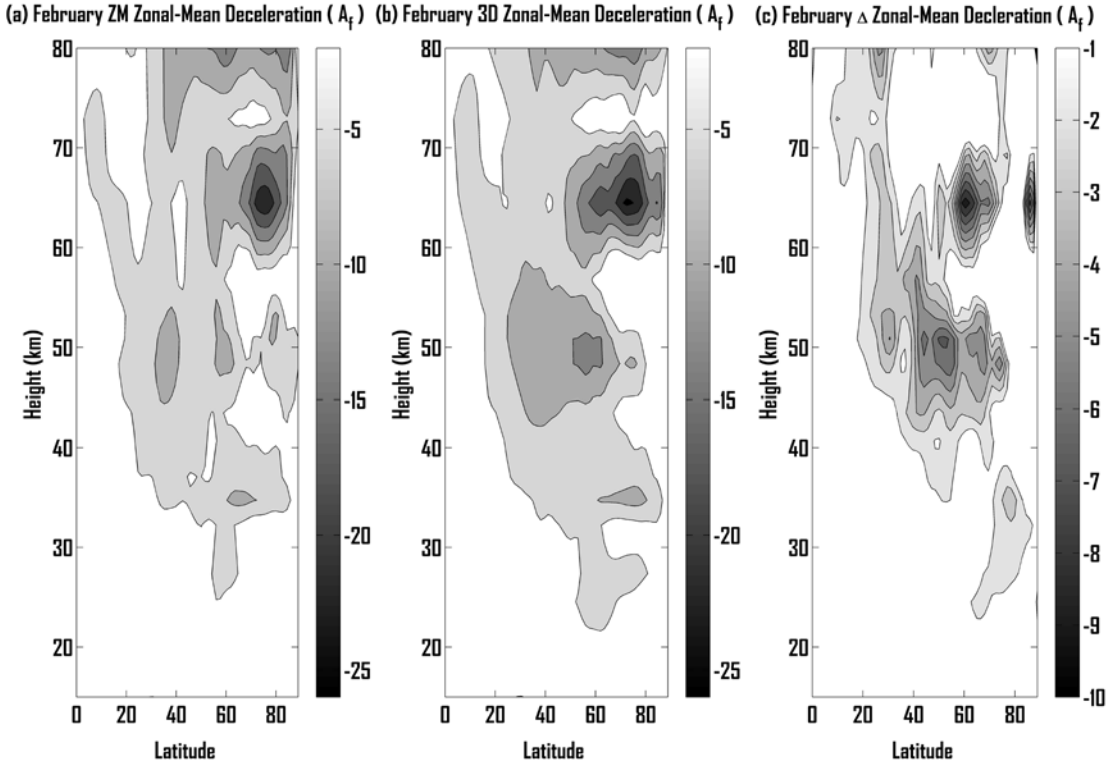


Figure 5. Contours of monthly averaged zonal-mean deceleration (A_f) in February for: (a) ZMO3; (b) 3DO3; and (c) the difference (3DO3 minus ZMO3). The contour interval is $4 \times 10^5 \text{ ms}^{-2}$.